



ELSEVIER

Infrared Physics & Technology 42 (2001) 479–484

INFRARED PHYSICS
& TECHNOLOGY

www.elsevier.com/locate/infrared

InAs/Al_xGa_{1-x}As quantum dot infrared photodetectors with undoped active region

Z.H. Chen^a, O. Baklenov^a, E.T. Kim^a, I. Mukhametzhanov^a, J. Tie^a,
A. Madhukar^{a,*}, Z. Ye^b, J.C. Campbell^b

^a Photonic Materials and Devices Laboratory, Departments of Materials Science and Physics, University of Southern California, VHE 506, 3651 Watt Way, Los Angeles, CA 90089-0241, USA

^b Microelectronics Research Center, Department of Electrical Engineering, The University of Texas at Austin, Austin, TX 78712, USA

Abstract

We report on a study of n-type quantum dot (QD) infrared photodetectors (QDIPs) based on InAs/GaAs QDs grown via an innovative technique called punctuated island growth. The electronic structure of the QDs inserted in QDIP devices is comprehensively investigated with photoluminescence, and intra- and interband photocurrent spectroscopy. The influence of AlGaAs layers inserted in active regions on the performance of the QDIPs is examined. Bias and temperature dependence of intraband photoresponse of QDIPs with undoped active region is examined. Initial results on intraband photoresponsivity and detectivity of these QDIPs at 77 K are reported. © 2001 Elsevier Science B.V. All rights reserved.

PACS: 73.50.Pz; 68.55.Bd; 78.66.Fd

Keywords: Quantum dot; Infrared photodetector; Intraband transition; Indium arsenide; Gallium arsenide; Photocurrent

Self-assembled semiconductor quantum dots (QDs) are particularly attractive candidates for middle- and long-wavelength (3–14 μm) infrared (IR) photodetectors due to their intrinsic sensitivity to normal incident IR light, the longer lifetime of excited electrons due to greatly suppressed electron–phonon scattering [1,2], and potentially significantly lower dark current [3,4]. The reported results on middle- and long-wavelength InAs/GaAs and InGaAs/GaAs quantum dot IR photodetectors (QDIPs) show promise [5–13]. The

QDIPs in these previous studies all had doped active regions. We studied n-type InAs QDIPs with both undoped and doped active InAs multiple QD regions. Our experimental results indicate that QDIPs with an undoped active region show smaller dark current than those with a doped active region. In this paper, we mainly focus on the QDIP structures with undoped active region. The electrons in the active InAs QDs are contributed from highly doped contact layers. The QDIPs reported here are based on GaAs-capped InAs QDs grown via the innovative technique called punctuated island growth (PIG) [14], which significantly narrows the PL line width of the inhomogeneous QD distribution down to ~25 meV.

* Corresponding author. Tel.: +1-213-740-4325; fax: +1-213-740-4333.

E-mail address: madhukar@ref.usc.edu (A. Madhukar).

The QDIP samples were grown on GaAs(001) $\pm 0.1^\circ$ substrates via solid-source molecular beam epitaxy. The InAs QDs were deposited at 500°C at a growth rate of 0.22 ML/s under As pressure of 7×10^{-6} Torr. GaAs cap layers were grown at 350°C via migration enhanced epitaxy to minimize intermixing between InAs and GaAs. This approach also enhances PL efficiency as compared with the usual MBE capping approach at the same growth condition [15]. An undoped active InAs QD region was inserted between highly Si-doped top and bottom GaAs contact layers and comprises a stack of five 3.0 ML InAs QDs grown via the PIG approach (2 ML + 60 s + 1 ML). The spacer between the bottom (top) contact layer and the nearest QD layer had a thickness of 220 (240) ML. The spacers between the active QDs have a thickness of 150 ML. In this paper, we present QDIPs with two kinds of spacer structures. In one structure, referred to as S-GaAs, the spacer material is GaAs. In another structure, referred to as S-AlGaAs, 21 ML AlAs/GaAs (1 ML/2 ML) short-period superlattices (SPSLs) are inserted to replace 21 ML of GaAs on both sides of each QD layer. The lower AlAs/GaAs SPSLs are located at a distance of 2 ML below the QD layer. The upper SPSLs are deposited after growth of a 30 ML GaAs capping layer above the QD layer. The AlAs/GaAs SPSLs are grown at 500°C via MEE approach, while the 30 ML capping GaAs is also grown via MEE but at 350°C.

Standard photolithography and wet chemical etching procedures were used for QDIP sample processing. The mesas have a diameter of 250 μm with alloyed AuGe/Ni/Au contacts. Inter and intraband photocurrent spectroscopy were performed with a Fourier transform IR (FTIR) spectrometer integrated with a cryostat and a current preamplifier. Spectral intraband responsivity was measured with a monochromatic spectrometer equipped with a Global source and a calibrated MCT IR photodetector. All photocurrent data were measured in the normal incident configuration. The bias polarity is relative to the grounded bottom contact. The noise characteristics were measured with both, an HP noise-figure meter and a lock-in preamplifier.

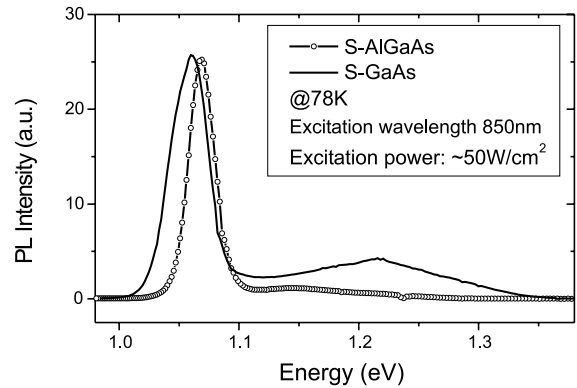


Fig. 1. PL spectra of S-GaAs and S-AlGaAs at 78 K.

The macroscopic defect density in these QDIPs is estimated to be $\sim 10^7 \text{ cm}^{-2}$ based on cross-sectional TEM measurements. PL spectra (Fig. 1) of the QDIP samples at 78 K show a main peak at 1.06 eV (S-GaAs) and 1.07 eV for (S-AlGaAs) and a small broad shoulder on the higher energy side. The main PL peak corresponds to the QD ground state transition. The small broad PL shoulder is most probably due to smaller QDs. The full-width at half-maximum (FWHM) of the main peak is 36 meV (25 meV) for S-GaAs (S-AlGaAs). The narrow PL line width enables us to get more information on the QD electronic structure. Systematic high-density PL and PL excitation (PLE) studies were performed on this class of QDs, and the electronic structures were identified [16].

Interestingly, interband transitions in these n-i(QD)-n QDIP structures are detected indicating that the electron ground state is not fully occupied. Fig. 2 shows a typical FTIR interband photocurrent spectrum on S-AlGaAs at a bias of +0.40 V at room temperature. Multiple peaks at 1.01, 1.10, 1.15, 1.20 and 1.27 eV are clearly resolved. If compared with the PL and PLE spectra (not shown here), the strongest peak at 1.01 eV can be attributed to the ground state transition of the QDs. The rest of the peaks can be attributed to excited states with excitation energy of 92, 140, 192, and 264 meV relative to the ground state. Although detailed transport mechanisms of interband photocurrent in QDIPs with n-i-n configuration are not very clear so far, it serves as a very

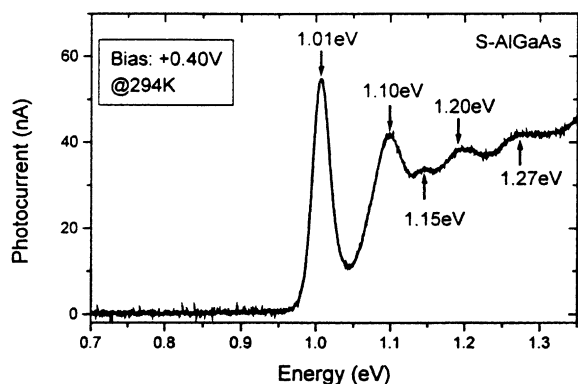


Fig. 2. Room temperature near IR interband photocurrent spectrum of S-AlGaAs (n-i-n configuration).

useful probe for QDIPs. The interband photocurrent spectroscopy is a complementary method to PLE and intraband photocurrent spectroscopy described below.

Intraband photocurrent spectroscopy offers more direct information on the QD electron states. Fig. 3a and b shows typical middle IR FTIR photocurrent spectra at 77 K for S-GaAs (at a bias of +0.4 V) and S-AlGaAs (at a bias of -1.00 V), respectively. The S-AlGaAs has a main intraband photoresponse peak at 205 meV (6.0 μm) with a FWHM of 16 meV, while S-GaAs has a main intraband photoresponse peak at 175 meV (7.2 μm) with a FWHM of 32 meV. Also S-GaAs shows a small intraband peak at 115 meV (10.8 μm). The addition of the AlGaAs layers leads to a blueshift in the wavelength of peak intraband photoresponse. This blue shift is attributed to an enhanced potential confinement by the inserted AlGaAs layers (as confining layer) as well as to a slight reduction in QD size (as estimated based on AFM data). A systematic PL/PLE study on single layer InAs/GaAs QD samples suggests that 300 ± 50 meV is the localization energy of the QD electron ground state [16]. Thus, the above-mentioned intraband transitions at 115 and 175 meV are bound-to-bound transitions. Fig. 4a and b shows bias-dependent intraband peak photoresponse for S-GaAs and S-AlGaAs at 77 K. Both show similar bias-dependent behavior. With increasing bias, the intraband photoresponse slowly increases at lower bias. Beyond a certain bias (~ 0.4 V for S-GaAs

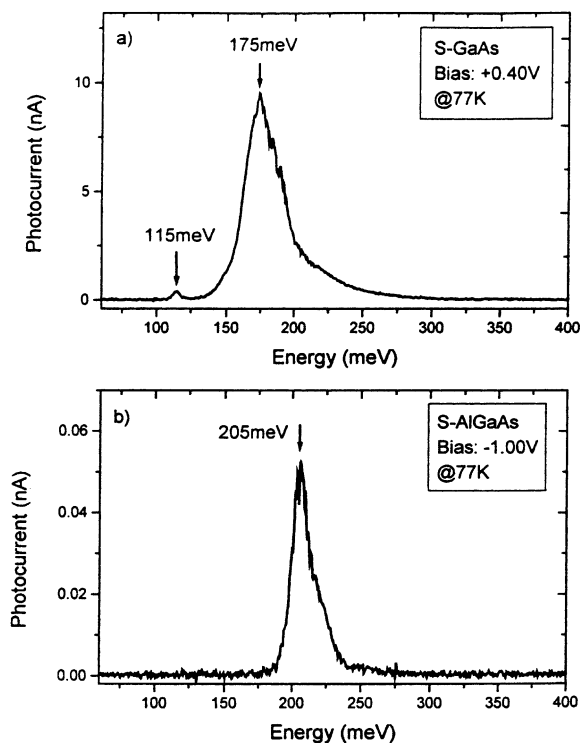


Fig. 3. Intraband photocurrent spectra of (a) S-GaAs and (b) S-AlGaAs at 77 K.

and ~ 1.0 V for S-AlGaAs), it increases rapidly. Namely, both structures show a threshold behavior. With further increase in bias, the photoresponse begins to drop, especially in S-GaAs. This is a negative differential photocurrent phenomenon. For S-GaAs, the intraband photoresponse at zero bias is small but not zero. The existence of this photovoltaic effect implies the presence of a permanent dipole, between QD electronic states, which originates from the intrinsically asymmetrical potential. (Following our observation of the permanent dipole moment and its suggested origin in the underlying asymmetry of the confining potential, theoretical confirmation has been provided by Sun and Chang [17].) In addition, both samples show asymmetric bias dependence between positive and negative bias. Most probably, this is also due to the intrinsically asymmetric QD potential. Temperature-dependent measurements reveal that both QDIPs show maximum intraband photoresponse at ~ 77 K.

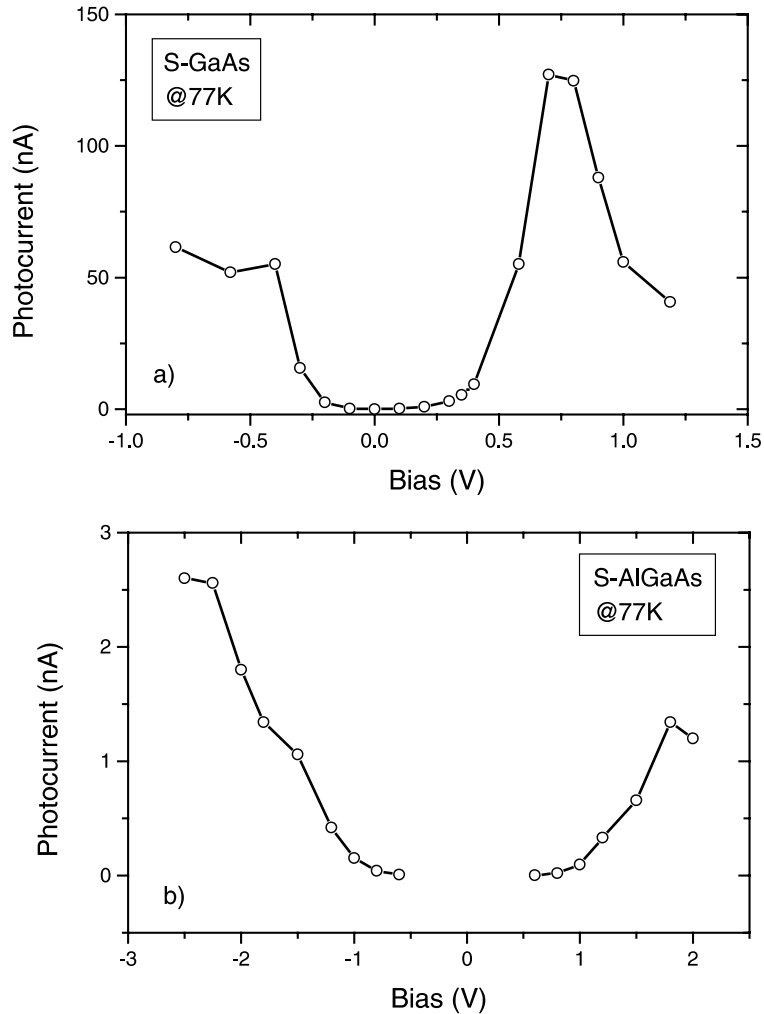


Fig. 4. Bias-dependent intraband peak photoresponse of (a) S-GaAs and (b) S-AlGaAs at 77 K.

Fig. 5 shows the dark current of S-GaAs and S-AlGaAs at 77 K. The dark current density of S-AlGaAs is dramatically decreased, up to 10^6 times (from 1 to 10^{-6} A/cm²), as compared with that of S-GaAs. This clearly indicates that the AlGaAs barriers added to the QDIP active region act as blocking layers [18] for the dark current. The impact of the AlGaAs layer on the photocurrent to dark current ratio is shown in Fig. 6. Within the measured bias range for each sample, the photocurrent to dark current ratio decreases nearly exponentially with increasing bias. The insertion of AlGaAs blocking layers in the QDIP leads to an

improvement of up to 10^3 times. This is due to the facts that the reduction of photocurrent by the AlGaAs blocking layer is smaller than that of dark current, and that the QD area is only about 20% of the wetting layer area. Initial measurements on S-GaAs show, at 77 K, an intraband peak photoresponsivity of ~ 1 A/W and peak detectivity larger than 10^9 cm Hz^{1/2}/W for a bias range of ± 0.2 V to ± 0.5 V. This result indicates that QDIPs with undoped active region are feasible.

In summary, we have systematically studied the characteristics of InAs/GaAs as well as InAs/GaAs/AlGaAs/GaAs QDIPs with undoped active

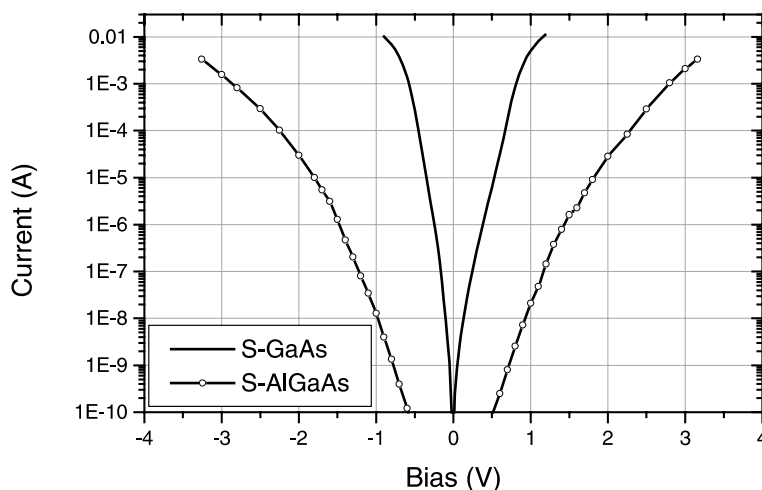


Fig. 5. Dark current (with room temperature background radiation) of S-GaAs and S-AlGaAs at 77 K.

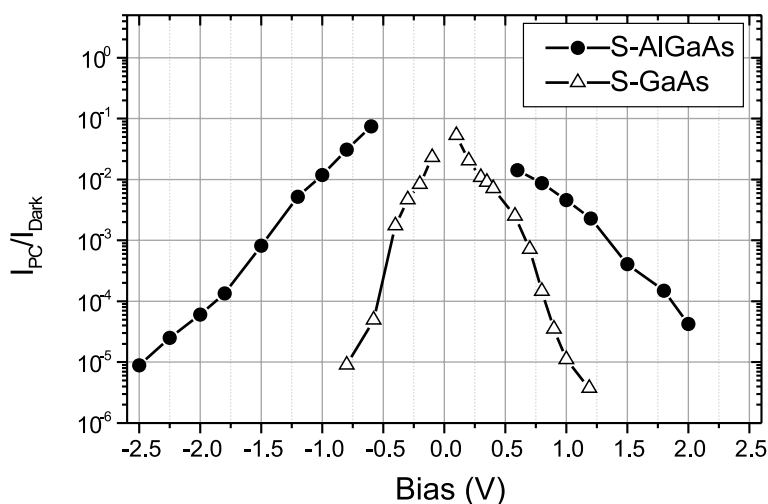


Fig. 6. Photocurrent to dark current ratio (I_{PC}/I_{Dark}) of S-GaAs and S-AlGaAs at 77 K.

regions consisting of a unique class of QDs grown via the PIG approach. The electronic structure of the InAs QDs embedded in QDIP structures has been comprehensively investigated with PL, PLE [16], and intra- and interband photocurrent spectroscopy. Our results show that appropriately designed InAs/AlGaAs QDIPs can serve as a sensor simultaneously for near IR ($\sim 1 \mu\text{m}$) and middle IR radiation. An AlGaAs layer inserted in the active

region of QDIPs can serve as a confining layer as well as a blocking layer. The intraband photoreponse peaks at 115 meV ($10.8 \mu\text{m}$) and 175 meV ($7.2 \mu\text{m}$) correspond to bound-to-bound transitions. A line width of the QDIP intraband photoreponse as narrow as 16 meV ($0.5 \mu\text{m}$) has been achieved. The QDIPs with undoped active region show a maximum intraband photoreponse at ~ 77 K. The initial intraband photoreponsivity and

detectivity results on the QDIPs at 77 K show attractive potential for IR sensor applications.

Acknowledgements

This work was supported by AFSOR under the MURI program on Nanoscience.

References

- [1] U. Bockelmann, G. Bastard, *Phys. Rev. B* 42 (1990) 8947.
- [2] H. Benisty, C.M. Sotomayer-Torrès, C. Weisbuch, *Phys. Rev. B* 44 (1991) 10945.
- [3] V. Ryzhii, *Semicond. Sci. Technol.* 11 (1996) 759.
- [4] D.M.-T. Kuo, A. Fang, Y.C. Chang, *Infrared Phys. Technol.* 42 (2001) 433.
- [5] S. Maimon, E. Finkman, G. Bahir, S.E. Schacham, J.M. Garcia, P.M. Petroff, *Appl. Phys. Lett.* 73 (1998) 2003.
- [6] D. Pan, E. Towe, S. Kennerly, *Appl. Phys. Lett.* 73 (1998) 1937.
- [7] D. Pan, E. Towe, S. Kennerly, *Appl. Phys. Lett.* 75 (1999) 2719.
- [8] D. Pan, E. Towe, S. Kennerly, *Appl. Phys. Lett.* 76 (2000) 3301.
- [9] S.J. Xu, S.J. Chua, T. Mei, X.C. Wang, X.H. Zhang, G. Karunasiri, W.J. Fan, C.H. Wang, J. Jiang, S. Wang, X.G. Xie, *Appl. Phys. Lett.* 73 (1998) 31.
- [10] Q.D. Zhuang, J.M. Li, H.X. Li, Y.P. Zeng, L. Pan, Y.H. Chen, M.Y. Kong, L.Y. Lin, *Appl. Phys. Lett.* 73 (1998) 3706.
- [11] S.-W. Lee, K. Hirakawa, Y. Shimada, *Appl. Phys. Lett.* 75 (1999) 1428.
- [12] L. Chu, A. Zrenner, G. Böhm, G. Abstreiter, *Appl. Phys. Lett.* 75 (1999) 3599.
- [13] J. Phillips, P. Bhattacharya, S.W. Kennerly, D.W. Beekman, M. Dutta, *IEEE J. Quant. Electron.* 35 (1999) 936.
- [14] I. Mukhametzhanov, Z. Wei, R. Heitz, A. Madhukar, *Appl. Phys. Lett.* 75 (1999) 85.
- [15] Q. Xie, P. Chen, A. Kalburge, T.R. Ramachandran, A. Nayfonov, A. Konkar, A. Madhukar, *J. Cryst. Growth* 150 (1995) 357.
- [16] I. Mukhametzhanov, Z.H. Chen, O. Baklenov, E.T. Kim, A. Madhukar, *Proceeding of International Conference on Semiconductor Quantum Dots, QD2000, Munich, Germany, August 2000, Phys. Status Solidi (b)* 224 (2001) 697.
- [17] S.J. Sun, Y.C. Chang, *Phys. Rev. B* 62 (2001) 13631.
- [18] O. Baklenov, Z.H. Chen, E.T. Kim, I. Mukhametzhanov, A. Madhukar, F. Ma, Z. Ye, B. Yang, J. Campbell, *The 58th IEEE Device Research Conference, Denver, CO, 19–21 June, 2000*, p. 171.